J. Fluid Mech. (1980), *vol.* 98, *part* 4, *pp.* 769–785
Printed in Great Britain

Double-diffusive instability in an inclined fluid layer Part 2. Stability analysis

By R. C. PALIWAL† AND C. F. CHEN
Department of Mechanical, Industrial and Aerospace Engineering,
Rutgers University, New Brunswick, New Jersey 08903

(Received 21 May 1979 and in revised form 18 October 1979)

Linear stability analysis is applied to the problem of a density-stratified fluid contained in an inclined slot being subjected to a lateral temperature gradient. Stability equations are solved using the Galerkin technique with 12 terms in the truncated expansion series. Within the range of θ considered, $|\theta| < 75°$, critical instability was found to be of the stationary type. Results of critical thermal Rayleigh numbers and wavenumbers at all inclination angles are in good agreement with the experimental results obtained earlier (Paliwal & Chen 1980). Contrary to intuition, these results show that the system is more stable when the lower wall is heated. This is shown to be the result of the increased vertical solute gradient in the steady state prior to the onset of instabilities when the heating is from below.

1. Introduction

In a companion paper (Paliwal & Chen 1980, hereinafter referred to as I) we reported the results of a series of experiments conducted in a stratified fluid contained in a narrow tank. The tank could be set at any angle of inclination with respect to the vertical, and a constant temperature difference could be maintained across the tank. We have obtained the critical thermal Rayleigh numbers and wavenumbers through a range of angles of inclination θ from $-75°$ to $+75°$. Negative angles denote heating of the upper wall and positive angles denote heating of the lower wall. The results show that the system is more stable when heating is from below, and the wavenumber decreases as $|\theta|$ increases. In this paper the results of a linear stability analysis of the problem are reported.

The convective stability of an inclined homogeneous fluid layer was investigated by Hart (1970, 1971*a*) both experimentally and theoretically. He found that, for

$$10° < |\theta| < 90°,$$

the instabilities were longitudinal rolls while, for $|\theta| < 10°$, the instabilities were transverse rolls.

The stability of a vertical layer of stratified fluid subjected to lateral temperature gradient was first treated by Thorpe, Hutt & Soulsby (1969). They did a simplified stability analysis in which the non-diffusive nature of the walls and the slow boundary-layer flows along the two walls were ignored. These approximations become better as

† Present address: Electronic Associates, Inc., West Long Branch, N.J. 07764.

0022-1120/80/4466–1160 $02.00

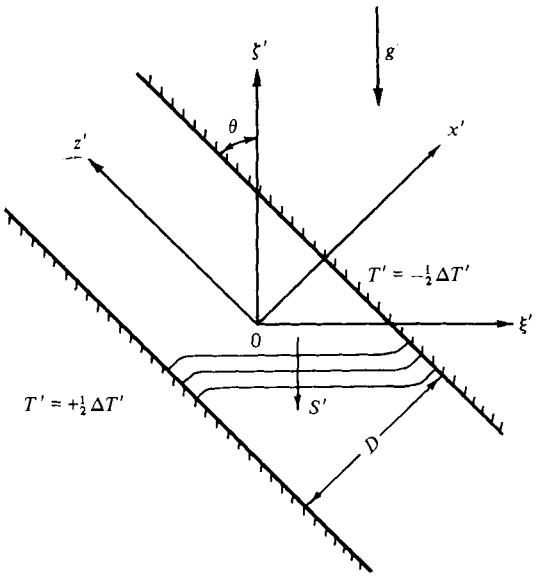

FIGURE 1. Co-ordinate system.

the solute Rayleigh number R_s becomes very large. The results of their stability analysis agreed quite well with their experimental results, which were obtained at large values of R_s.

Hart's (1971*b*) analysis of the same problem accounted for both the actual basic velocity field and boundary conditions. By the use of the Galerkin technique he found critical conditions for a range of values of R_s. His results at large R_s were indistinguishable from those of Thorpe *et al.* By making a finite-amplitude study of the problem, Hart (1973) was able to improve the agreement between the theoretical results with the experimental results of Thorpe *et al.*

In this paper, we report solution of the stability equations using the Galerkin method. Our expansion functions are essentially the same as those used by Hart (1971*b*), with one important difference. In the expansion for the salinity S, a constant term is added. The boundary conditions on S are preserved since they involve only normal derivatives. For the vertical geometry, our results differ only slightly from those of Hart (1971*b*). However, for cases in which $\theta \neq 0°$, erroneous results would be obtained if the constant term were neglected.

2. Governing equations

Figure 1 shows schematically the inclined fluid layer bounded between rigid parallel walls which are a small distance D apart. The walls are infinitely long in the z direction and are inclined at θ from the vertical. There is a stable linear density gradient

$$\phi_0 = |\rho'^{-1} d\rho'/d\zeta|_0 \,(\mathrm{cm}^{-1})$$

due to the solute in the vertical direction. The constant-solute-concentration lines, which are horizontal in most of the interior region, curve near the sloping boundaries in order to meet the boundaries normally as required by the non-diffusive boundary

conditions. The temperature gradient, which is also linear, is in the direction normal to the walls. The isotherms are thus parallel to the boundaries. The walls are perfect heat conductors and are maintained at constant temperatures. The temperature difference across the boundaries is ΔT.

The density of the fluid is

$$\rho' = \rho_0'[1 - \alpha(T' - T_0') + \beta(S' - S_0')], \tag{1}$$

where $$\alpha = -\frac{1}{\rho'}\left(\frac{\partial \rho'}{\partial T'}\right)_{p', S'}, \quad \beta = \frac{1}{\rho'}\left(\frac{\partial \rho'}{\partial S'}\right)_{p', T'};$$

T' and S' denote temperature and salinity respectively, while subscript 0 denotes reference values.

Assuming two-dimensional flow and using the Boussinesq approximation, the equations of motion are cross-differentiated to eliminate the pressure. The resulting vorticity (ω) equation in dimensionless form is

$$\frac{1}{Pr}\frac{D\omega}{Dt} = \nabla^2\omega - \cos\theta\left\{R_T\frac{\partial T}{\partial x} - R_S\frac{\partial S}{\partial x}\right\} + \sin\theta\left\{R_T\frac{\partial T}{\partial z} - R_S\frac{\partial S}{\partial z}\right\}, \tag{2}$$

where $$R_T = \frac{g\alpha\Delta T D^3}{\nu\kappa_T}, \quad R_S = \frac{g\beta|\partial S/\partial\zeta|_0 D^4}{\nu\kappa_T},$$

and $$Pr = \nu/\kappa_T.$$

The diffusion equations for heat and salt are

$$\frac{DT}{Dt} = \nabla^2 T, \tag{3}$$

and $$\frac{DS}{Dt} = \frac{\kappa_S}{\kappa_T}\nabla^2 S. \tag{4}$$

In the above equations, g is the gravitational acceleration, κ_s and κ_t are the diffusivities of salt and heat respectively. These equations are rendered dimensionless by using D, D^2/κ_T, ΔT and $D|dS/d\zeta|_0$ as characteristic length, time, temperature and salinity, respectively.

2.1. *Basic flow*

For an infinitely long slot, the basic flow is parallel to the boundaries with

$$\omega = -dw/dx.$$

Further, there is no temperature gradient in the z direction and the non-dimensional solute gradient in the z direction is constant and equal to $-\cos\theta$. Equations describing the steady basic flow thus are

$$\frac{d^3w}{dx^3} + \cos\theta\left[R_T\frac{dT}{dx} - R_S\frac{dS}{dx}\right] - R_S\sin\theta\cos\theta = 0, \tag{5}$$

$$\frac{d^2T}{dx^2} = 0, \tag{6}$$

and $$\frac{d^2S}{dx^2} + \left(\frac{\kappa_T}{\kappa_S}\cos\theta\right)w = 0. \tag{7}$$

These equations may be combined into a single equation:

$$\frac{d^4w}{dx^4} + (4K^4)\,w = 0, \tag{8}$$

where $$K = \left(\frac{1}{4}\frac{\kappa_T}{\kappa_S} R_S \cos^2\theta\right).$$

The boundary conditions are

$$w = 0, \quad \frac{d^3w}{dx^3} = R_S(\sin\theta + R_T)\cos\theta \quad \text{at} \quad x = \pm\tfrac{1}{2}. \tag{9}$$

The steady-state solution is

$$w_b = \frac{G}{2K^3(\sin K + \sinh K)}\left[\sinh\left(Kx+\frac{K}{2}\right)\sin\left(Kx-\frac{K}{2}\right) - \sin\left(Kx+\frac{K}{2}\right)\sinh\left(Kx-\frac{K}{2}\right)\right], \tag{10}$$

$$T_b = -x, \tag{11}$$

$$\frac{dS_b}{dx} = \frac{\kappa_T}{\kappa_S}\cos\theta\frac{G}{2K^3(\sin K+\sinh K)}\left[\frac{1}{2K}\left\{\cosh\left(Kx+\frac{K}{2}\right)\sin\left(Kx-\frac{K}{2}\right) - \sinh\left(Kx+\frac{K}{2}\right)\cos\left(Kx-\frac{K}{2}\right)\right\} - \frac{1}{2K}\left\{\cosh\left(Kx-\frac{K}{2}\right)\sin\left(Kx+\frac{K}{2}\right) - \sinh\left(Kx-\frac{K}{2}\right)\cos\left(Kx+\frac{K}{2}\right)\right\}\right] - \frac{\kappa_T}{\kappa_S}\cos\theta\left(\frac{G}{4K^4}\right), \tag{12}$$

where $G = [R_T + R_S\sin\theta]\cos\theta$.

Steady-state basic velocity fields evaluated at the mean experimental condition with $Pr = 6{\cdot}7$, $\kappa_T/\kappa_S = 83$ and $R_S = 362\,000$ for $\theta = 0°$, $\pm 30°$ and $\pm 60°$ are shown for $R_T = 0$ and 100 000 in figure 2. In the absence of heating ($R_T = 0$), there is no flow at all if the boundaries are vertical. When the slot is inclined, the flow is always up the lower wall and down the upper wall, its magnitude increasing with inclination θ. For negative values of θ, the upper wall corresponds to $x = 0$. The effect of heating ($R_T = 100\,000$) is always an upward flow near the hot wall and a downward flow near the cold wall. For positive angles, therefore, heating (from below) results in further increase of the already upward flow near the lower boundary. In the case of negative angles, the effect of heating (from above) is to decrease the magnitude of the velocity, with possible reversal of its direction if heating is increased. In general, at a given R_T and θ, a velocity field of higher magnitude exists for the case of heating from below compared to that of heating from above. The velocity field is always confined to a region extending only about a tenth or so of the slot width near the walls. The peak velocity occurs about halfway in this small region, and its typical value at $\theta = 60°$ and $R_T = 100\,000$ is about 10^{-3} cm s^{-1}. Most of the interior region has no motion. The distribution of velocity in the slot is antisymmetric in the x direction.

Figure 3 shows the basic steady-state solute gardient dS_b/dx at $\theta = 0°$, $\pm 30°$ and $\pm 60°$ for $R_T = 0$ and $R_T = 100\,000$. In most of the interior region, dS_b/dx has a constant value for a given θ and R_T. In the absence of heating, dS_b/dx assumes the value $(-\sin\theta)$ in the interior as a result of initial vertical stratification. In the buoyancy

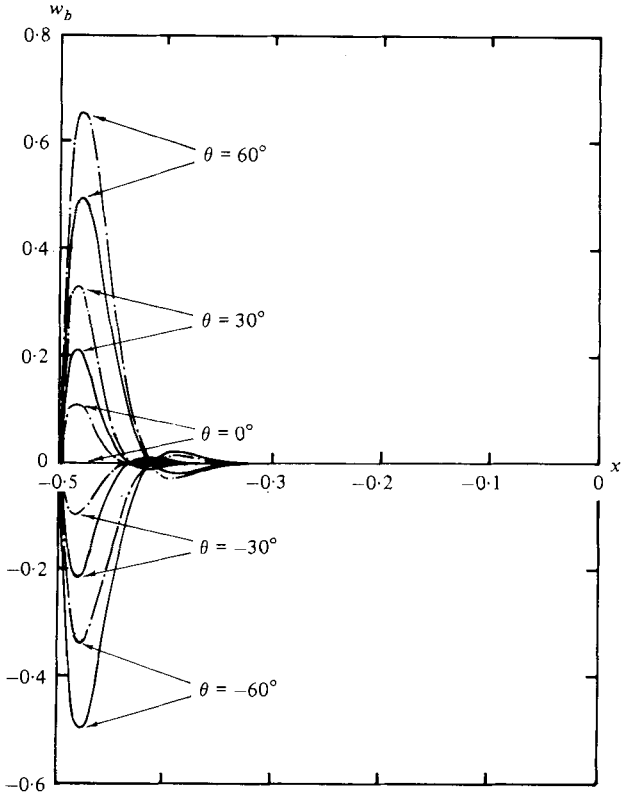

FIGURE 2. Steady-state velocity for $Pr = 6{\cdot}7$, $\kappa_T/\kappa_S = 83$ and $R_S = 362\,000$. ——, $R_T = 0$; —·—, $R_T = 100\,000$.

layer, dS_b/dx increases from zero at the boundary to a peak value not far from the wall, and then decreases to a constant value in most of the interior. The effect of heating is additive for positive inclinations and subtractive for negative inclinations, in the buoyancy layer as well as in the main interior. The magnitude of the gradient dS_b/dx, at a given θ and R_T, is higher for the heating-from-below case compared to that of heating from above. The dS_b/dx profile is always symmetrical in the x direction.

2.2. *Linear stability equations*

Since the secondary flows observed in the experiments of I are periodic in the vertical direction, we assume all perturbations are periodic in z with a wavenumber k. These are

$$u(x)\exp(ikz+pt), \quad \text{etc.},$$

with p complex. When these perturbation quantities are substituted into the basic equations, retaining only linear terms we obtain the following equations written in terms of the perturbation stream function ψ, where

$$\frac{\partial\psi}{\partial x} = w, \quad \frac{\partial\psi}{\partial z} = -u:$$

$$-\frac{p}{Pr}(d^2-k^2)\psi + (d^2-k^2)^2\psi - \frac{ik}{Pr}\{w_b(d^2-k^2)\psi - \psi d^2 w_b\}$$
$$+\cos\theta(R_T\,dT - R_S\,dS) - ik\sin\theta(R_T\,T - R_S\,S) = 0, \quad (13)$$

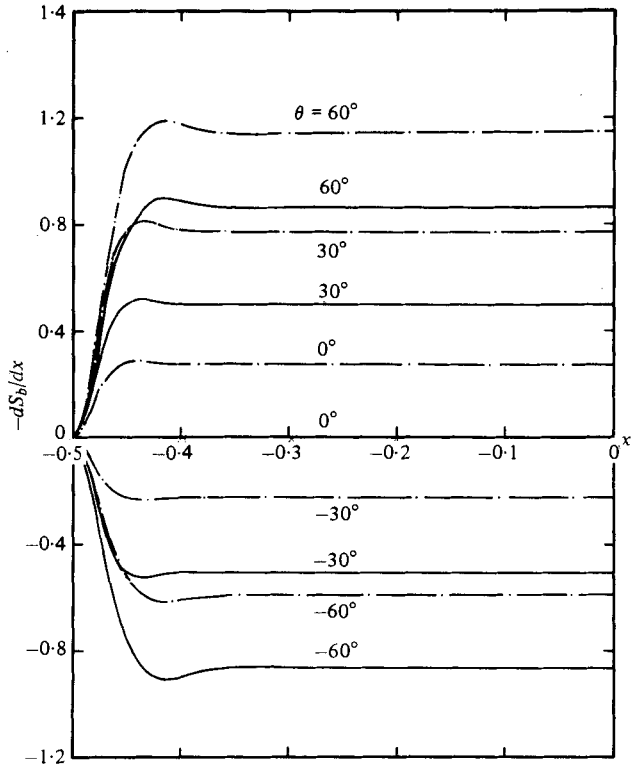

FIGURE 3. Steady-state solute gradient for $Pr = 6{\cdot}7$, $\kappa_T/\kappa_S = 83$ and $R_S = 362000$.

$$-pT + (d^2 - k^2)\,T - ik\psi - ikw_b T = 0, \tag{14}$$

$$-\frac{\kappa_T}{\kappa_S} pS + (d^2 - k^2)\,S + ik\psi\left(\frac{\kappa_T}{\kappa_S}\right) dS_b - ik\left(\frac{\kappa_T}{\kappa_S}\right) w_b S + \left(\frac{\kappa_T}{\kappa_S}\right) \cos\theta\, d\psi = 0. \tag{15}$$

The boundary conditions are

$$\psi = d\psi = T = dS = 0 \quad \text{at} \quad x = \mp\tfrac{1}{2}. \tag{16}$$

In these equations, d denotes d/dx. When $\theta = 0$ these equations reduce to those analysed by Hart (1971*b*).

3. Method of solution

The stability equations (13)–(15) are a set of ordinary linear differential equations of total order 8. These, together with the boundary conditions (16), are solved using the Galerkin method. Finlayson (1972) has reviewed applications of the Galerkin method to a number of convective instability problems. Stability of pure thermal convection between sloping boundaries and double-diffusive convection in a vertical slot has been studied, using this technique, by Hart (1970, 1971*a*, *b*). The success of this method in these two investigations as well as a number of others (see Finlayson 1972) provides the necessary impetus for its use in the present problem of double-diffusive convection in an inclined slot.

In principle, the Galerkin method is a special case of the more general method called the method of weighted residuals (MWR), which is a technique to obtain approximate solutions of higher-order differential equations. In the MWR, the unknown solution is expanded in a set of appropriately chosen trial functions with adjustable constants (or functions). These constants or functions are then determined so as to give the best solution of the system of differential equations. To do so, the assumed solution is substituted in the system of differential equations, and the residuals, appropriately weighted, are set to zero in some average sense to give the best values of the unknown constants or functions. In the Galerkin method, the trial functions chosen form a complete set, and the trial functions themselves are used as weighting functions. In other words, the residuals are made orthogonal to the respective trial functions.

It is convenient if the trial functions chosen satisfy the boundary conditions of the problem. A common approach (Finlayson 1972) is to choose the eigenfunctions of some simpler version of the eigenvalue problem under consideration as trial functions. Such a simpler eigenvalue problem, corresponding to equation (13), is

$$d^4\psi = \lambda^4\psi,$$

with boundary conditions $\psi = d\psi = 0$ at $x = \mp \frac{1}{2}$. The appropriate trial functions are then the following.

Even function:

$$E_n = \frac{\cosh(\rho_n x)}{\cosh \frac{1}{2}\rho_n} - \frac{\cos(\rho_n x)}{\cos \frac{1}{2}\rho_n} \quad \text{if} \quad n \text{ is odd},$$

where

$$\tanh \tfrac{1}{2}\rho_n + \tan \tfrac{1}{2}\rho_n = 0.$$

Odd function: $$O_n = \frac{\sinh(\mu_n x)}{\sinh \frac{1}{2}\mu_n} - \frac{\sin(\mu_n x)}{\sin \frac{1}{2}\mu_n} \quad \text{if} \quad n \text{ is even},$$

where

$$\coth \tfrac{1}{2}\mu_n - \cot \tfrac{1}{2}\mu_n = 0.$$

Following a similar reasoning, the trial functions for temperature T and solute concentration S are the ordinary trigonometric functions satisfying the appropriate boundary conditions.

The solutions expressed in terms of the trial functions chosen are:

$$\psi = \sum_{n=1}^{N} a_n \psi_n, \tag{17}$$

where

$$\psi_n = \begin{cases} E_n & \text{if} \quad n \text{ is odd}, \\ O_n & \text{if} \quad n \text{ is even}; \end{cases}$$

$$T = \sum_{n=1}^{N} b_n T_n, \tag{18}$$

where

$$T_n = \begin{cases} \cos n\pi x & \text{if} \quad n \text{ is odd}, \\ \sin n\pi x & \text{if} \quad n \text{ is even}; \end{cases}$$

and

$$S = c_1 + \sum_{n=2}^{N} c_n S_n, \tag{19}$$

where

$$S_n = \begin{cases} \sin(n-1)\pi x & \text{if} \quad n \text{ is even}, \\ \cos(n-1)\pi x & \text{if} \quad n \text{ is odd}. \end{cases}$$

It may be noted that the trial functions chosen form a complete set, are orthogonal and satisfy the boundary conditions of the problem.

The next step is to determine the coefficients a_n, b_n and c_n in equations (17)–(19). This is done by substituting equations (17)–(19) into the stability equations (13)–(15) and operating the residual equations by

$$\int_{-\frac{1}{2}}^{\frac{1}{2}} \psi_j \, dx, \quad \int_{-\frac{1}{2}}^{\frac{1}{2}} T_j \, dx \quad \text{and} \quad \int_{-\frac{1}{2}}^{\frac{1}{2}} S_j \, dx,$$

respectively. The result is a system of simultaneous algebraic equations which, in matrix form, are

$$\left[\begin{bmatrix} A_{11} & A_{12} & A_{13} \\ A_{21} & A_{22} & A_{23} \\ A_{31} & A_{32} & A_{33} \end{bmatrix} - p \begin{bmatrix} B_{11} & 0 & 0 \\ 0 & B_{22} & 0 \\ 0 & 0 & B_{33} \end{bmatrix}\right] \begin{bmatrix} \mathbf{a} \\ \mathbf{b} \\ \mathbf{c} \end{bmatrix} = 0, \tag{20}$$

where the elements A_{ji} and B_{ji} are sub-matrices involving integrals of products of perturbation quantities and products of the basic flow quantities; for details see Paliwal (1979). The integrals which do not involve the basic state can be evaluated exactly. The integrals involving the basic state are evaluated numerically by using the Scientific Subroutine Package DQSF based on Simpson's rule and available on System IBM 370/168. A 21-point mesh between $x = -\frac{1}{2}$ and $x = +\frac{1}{2}$ is used. A higher number of mesh point does not result in any additional accuracy.

Equation (20) writen in a more compact form is

$$(\mathbf{A} - p\mathbf{B})\,\mathbf{X} = 0, \tag{21}$$

where $\mathbf{X}$ is the vector made up of coefficients $\mathbf{a}$, $\mathbf{b}$ and $\mathbf{c}$, $\mathbf{A}$ and $\mathbf{B}$ are $3(m-1) \times 3(m-1)$ matrices with complex elements. Premultiplication of equation (21) by $\mathbf{B}^{-1}$ gives

$$(\mathbf{B}^{-1}\mathbf{A} - p\mathbf{I})\,\mathbf{X} = 0, \tag{22}$$

where $\mathbf{I}$ is the unit matrix.

It is recalled that the elements of matrices $\mathbf{A}$ and $\mathbf{B}$ are functions of parameters R_S, R_T, Pr, θ, κ_T/κ_S and k. For a given set of values of these parameters, solution of equations (22) amounts to the determinations of eigenvalues of the complex matrix $\mathbf{B}^{-1}\mathbf{A}$. For a non-trivial solution of equations (22),

$$\det(\mathbf{B}^{-1}\mathbf{A} - p\mathbf{I}) = 0. \tag{23}$$

As noted earlier, p, in general, is complex and has the form

$$p = p_{\mathrm{Re}} + ip_{\mathrm{Im}}. \tag{24}$$

For marginal instability, $p_{\mathrm{Re}} = 0$. Further, $p_{\mathrm{Im}} = 0$ for stationary instability and $p_{\mathrm{Im}} \neq 0$ for oscillatory instability.

It is convenient to assume $p_{\mathrm{Im}} = 0$ and determine, first, the marginal stationary instability ($p = p_{\mathrm{Re}} = p_{\mathrm{Im}} = 0$). It is done by finding, for given values of R_S, θ, Pr and κ_T/κ_S, zeros of the equation

$$\det(\mathbf{B}^{-1}(R_T, k)\,\mathbf{A}(R_T, k)) = 0, \tag{25}$$

or
$$\det(\mathbf{B}^{-1}(R_T, k)).\det(\mathbf{A}(R_T, k)) = 0,$$

or
$$\det(\mathbf{A}(R_T, k)) = 0,$$

as
$$\det(\mathbf{B}^{-1}(R_T, k)) \neq 0 \quad \text{if } \mathbf{B}^{-1} \text{ exists.}$$

Equation (25) is a polynomial of degree $3(m-1)$ in R_T and k. For a given value of wavenumber k, $3(m-1)$ values of R_T are possible and vice versa. The minimum value of R_T and the corresponding k is the critical wavenumber. For arbitrary discrete values of R_T and k, the determinant of $\mathbf{A}$ is computed. For a given k, a change in sign of the determinant owing to an increment in R_T indicates a zero of the determinant. An iteration procedure is used to determine the minimum R_T (critical) and the associated critical wavenumber.

After the critical values of R_T and k for stationary instability are determined, eigenvalues of the matrix $\mathbf{B}^{-1}\mathbf{A}$ are determined for the same values of parameters R_S, θ, Pr and κ_T/κ_S. At marginal instability, the real part of only one eigenvalue changes sign from negative (decaying disturbance) to positive (growing disturbance). If the accompanying imaginary part of this eigenvalue is non-zero, the instability is oscillatory; otherwise it is stationary. If at values of parameters R_T and k corresponding to the stationary instability there is more than one eigenvalue having positive real parts, subcritical oscillatory instabilities are possible and the search for the critical R_T is continued. The lowest R_T for any k, at which just one of the eigenvalues has a positive real part, corresponds, then, to critical R_T and the corresponding k is critical k. Subroutines LEQTIC and EIGCC of the IMSL library available on system IBM 370/168 are used to compute the determinants and the eigenvalues respectively.

Values of the critical parameter $R_{T,c}$ and k_c at the mean experimental conditions (see I) of $Pr = 6{\cdot}7$, $\kappa_T/\kappa_S = 83$ and $R_S = 362\,000$ at selected angles of inclination are calculated with N assuming values of 8, 10, 12, and 14. The results for $N = 12$ differ by less than 0·1 % from those for $N = 14$. It is therefore assumed that convergence is obtained for $N = 12$. It is noted that, even at $N = 8$, the values of $R_{T,c}$ are within 5 % and the values of k_c are within 10 % of those obtained with $N = 12$. The critical values obtained by theoretical considerations with $N = 12$ are compared with the experimental values obtained in I, §5.

4. Specialized known cases of the generalized problem

Several special cases of the present problem are already known. To give support to the theoretical analysis presented in the preceding sections, it is instructive to recover these cases from the generalized analysis and compare the results with earlier predictions.

4.1. *Special case of* $R_S = 0$ (*homogeneous fluid*)

In the limit of $R_S \to 0$, equation (10) for the basic velocity reduces to

$$w_b = \tfrac{1}{6} R_T \cos\theta [x^3 - \tfrac{1}{6}x].$$

This is the same as reported by Hart (1970, 1971*a*) for pure thermal convection in a narrow and long tilted slot (limit of pure conduction across the slot). With our calculations, $R_S = 0$ will involve a number of singular terms. To avoid this difficulty, we calculated the case $R_S = 1{\cdot}0$ for critical instability of the fluid at different tilt angles of the slot. The results are shown in figure 4, together with Hart's (1970) result corresponding to the exact limit of $R_S = 0$. These are all for transverse waves which derive their energy from the mean shear when $\theta < 60°$, and from the unstable temperature field for θ near 90°. The satisfactory approach of the full problem to zero solute stratification is obvious.

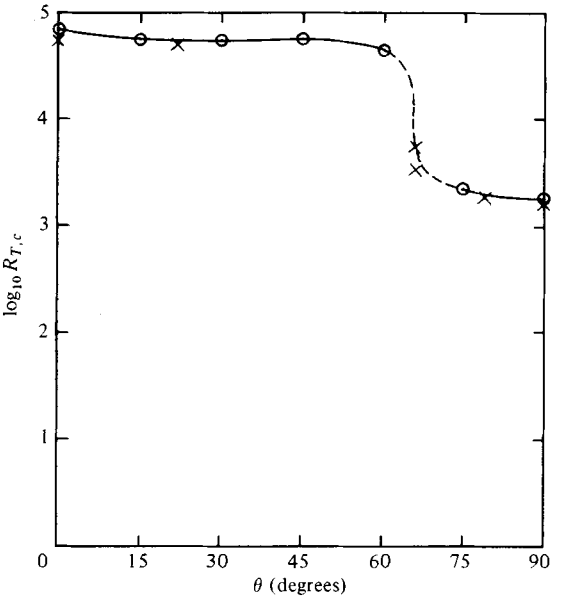

FIGURE 4. Critical thermal Rayleigh number for the inclined homogeneous fluid layer. ○, present results for $R_S = 1$; ×, Hart's (1970) results for $R_S = 0$. The dotted line indicates a possible variation of $R_{T,c}$ between 60° and 75°.

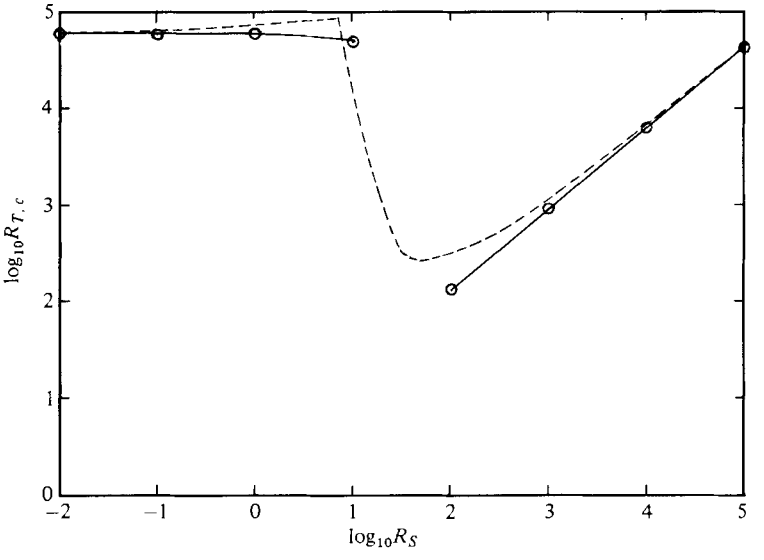

FIGURE 5. Critical thermal Rayleigh number for a vertical layer of stratified fluid. ○, present results; – – –, Hart (1971*b*). The present results are not connected between $R_S = 10$ and 100 because no calculations were made within this range.

4.2. *Special case of* $\theta = 0°$ (*vertical fluid layer*)

Double-diffusive stability criteria for vertical geometry have been reported by Hart (1971*b*) for a range of R_S from 0 to 10^5. Comparison of these with the corresponding results obtained in the manner of § 3 ($N = 8$) is shown in figures 5 and 6. As is already known, the critical instability is of the stationary type. Some disagreement is seen at

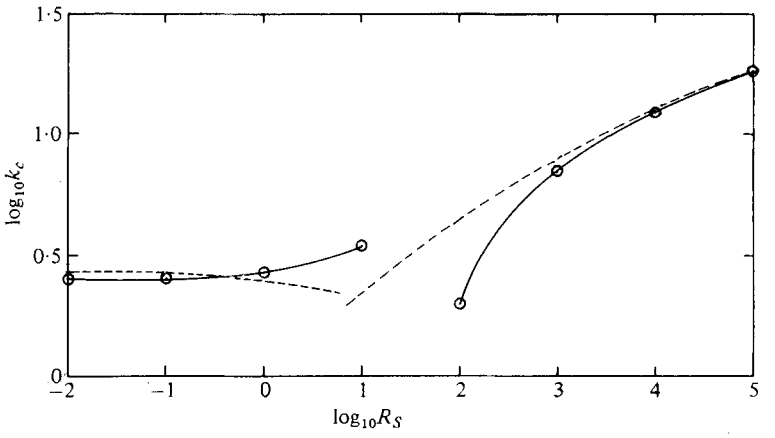

FIGURE 6. Critical wavenumber for a vertical layer of stratified fluid. See figure 5 for symbols and comments.

values of R_S between 10 and 100 which are low but sufficient for the sideways diffusive mechanism to be possible. The disagreement is due to a small difference in the choice of the trial functions for use in the Galerkin method between us and Hart. His expansion of the variable S in terms of trial functions did not include a constant leading term, as used in equations (19) here. This addition of a constant term is most crucial for values of $\theta + 0°$ as we have found that, without the constant term, the Galerkin method would yield much higher $R_{T,c}$ values. For high R_s, there is excellent agreement of the stability predictions of this work with previous theoretical and experimental investigations. In fact, the predictions of the present theory are in full agreement with the asymptotic relation of Thorpe *et al.* (1969).

4.3. *Special case of* $\theta = 90°$ (*horizontal fluid layer heated from below*)

It is to be noted that the theoretical model developed here is not suitable for the special case of $\theta = 90°$ (horizontal geometry). In the limit of $\theta = 90°$, equation (7), describing the basic steady-state solute distribution in the x direction, becomes

$$\frac{d^2S}{dx^2} = 0$$

with boundary conditions $dS/dx = 0$ at $x = \mp \frac{1}{2}$. The solution of this implies vertical constant-solute concentration lines, or no stabilizing vertical stratification.

In reality, an initially-linear stable vertical solute gradient in a thin horizontal fluid layer enclosed between rigid and impervious boundaries is not steady. It does, however, go to steady state of zero gradient rather slowly, in view of the small molecular diffusivities of most solutes. A crude and arbitrary approximation of the basic state corresponding to quasi-steady conditions which may exist in real experiments like those of Shirtcliffe (1969) is

$$w_b = 0, \quad dS_b/dx = -(\cos \pi x)^{0\cdot 03125}.$$

These equations satisfy the actual boundary conditions associated with rigid, heat-conducting and impervious boundaries. The gradient (figure 7) dS_b/dx is almost -1 everywhere except very close to the wall. It is interesting as well as encouraging that

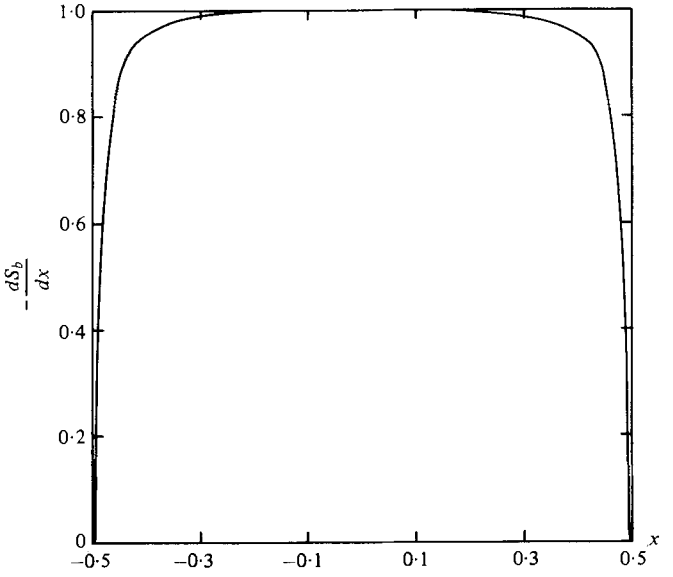

FIGURE 7. Assumed steady-state solute gradient at $\theta = 90°$.

computations made with this crude model of the basic state for $Pr = 6{\cdot}7$, $R_S = 362\,000$, $\kappa_T/\kappa_S = 101$ and $\theta = 90°$ predict oscillatory instability at $R_{T,c} = 323\,000$ and $k_c = 6{\cdot}54$. This $R_{T,c}$ is only 2·7 % higher than the predictions of Veronis (1965)

$$R_{T,c} = [Pr/(1+Pr)]\,R_S$$

for large values of R_S.

5. Results and discussion

The true measure of the success of the theoretical model is its ability to predict the experimental data obtained in I. The comparison of the experimental results with corresponding theoretical predictions for critical thermal Rayleigh number ($R_{T,c}$) and critical wavenumber (k_c) are shown in figures 8 and 9. The theoretical computations have been performed with $Pr = 6{\cdot}7$, $\kappa_T/\kappa_S = 83{\cdot}0$ and $R_S = 362\,000$, which correspond to average conditions of the experiments. Results have been obtained using the Galerkin method, with 12 terms in the truncated expansion series. These are tabulated in table 1. As stated in previous sections, $-\theta$ corresponds to heating from above and $+\theta$ corresponds to heating from below. Theoretical computations show that, for all angles in the range $-75° < \theta < +75°$, the critical instability is of the stationary type.

It may be observed that the trend of the $R_{T,c}, \theta$ curve as well as the k_c, θ curve is very well predicted by the theory. Both theory and experiment show that heating of the lower wall is more stable than heating of the upper wall. Experimental data generally fall above the theoretical curve in the case of $R_{T,c}$ and below it in the case of k_c. Theoretical $R_{T,c}$ has been calculated using R_S that corresponds to the measurements made about 1 or 2 h after filling the tank. There is continuous diffusion into and from the stratified region at the bottom and top respectively, due to the presence of homogeneous layers. The effect, if any, of this diffusion is to make the solute gradient in the stratified region steeper, thereby delaying instability. As θ increases, the effective

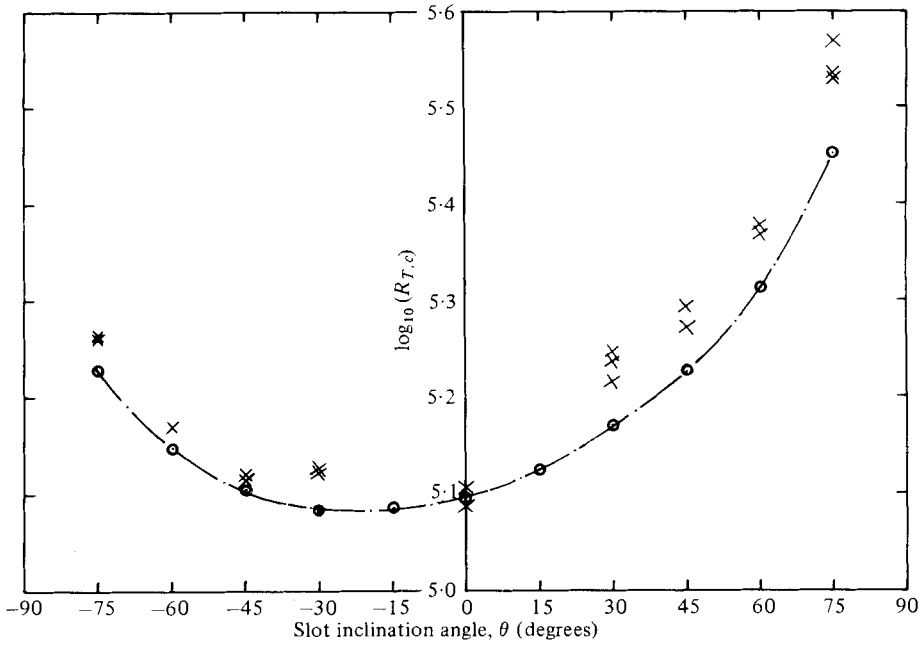

FIGURE 8. Comparison of theory with experiments: critical thermal Rayleigh number. ○, theory; ×, experiment.

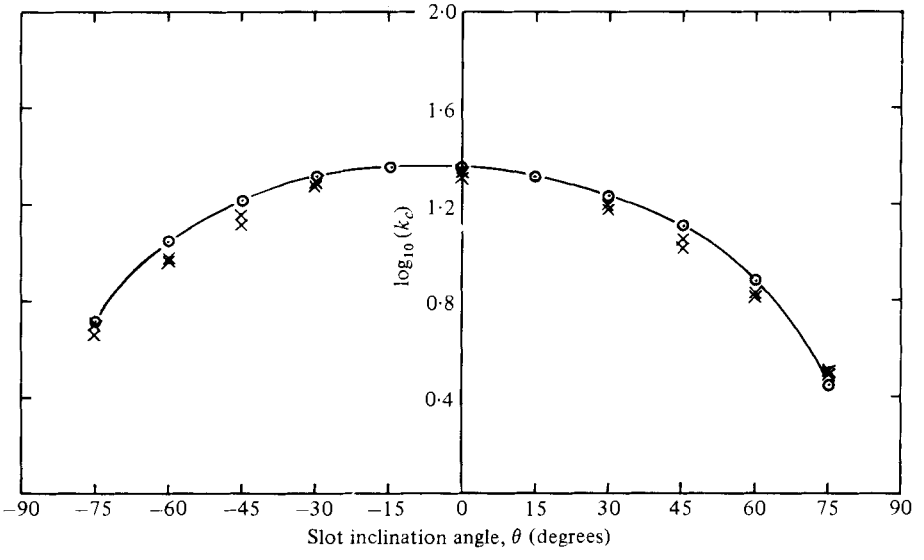

FIGURE 9. Comparison of theory with experiments: critical wavenumber. ○, theory; ×, experiment.

vertical height of the stratified region becomes less and the effect of diffusion at the bottom and the top becomes more pronounced. A steeper gradient delays instability until $R_{T,c}$ is slightly higher. This effect becomes more noticeable at higher values of $|\theta|$.

The fact that the experimental data for the wavenumber k_c are generally below the

Angle	$R_{T,c}$	k_c	$\log_{10} R_{T,c}$	$\log_{10} k_c$
−75°	169219	5·195	5·228	0·7156
−60°	139922	11·203	5·146	1·0493
−45°	127234	16·537	5·105	1·2185
−30°	121219	20·586	5·084	1·3136
−15°	122375	22·405	5·088	1·3503
0	124563	22·502	5·095	1·3522
+15°	133805	20·621	5·126	1·3143
+30°	148203	17·062	5·171	1·2320
+45°	169219	12·880	5·228	1·1099
+60°	205625	7·689	5·313	0·8858
+75°	283438	2·781	5·453	0·4442

Note: $\kappa_T/\kappa_S = 83$, $R_S = 362000$, $N = 12$.

TABLE 1. Summary of the theoretically computed results using the Galerkin method.

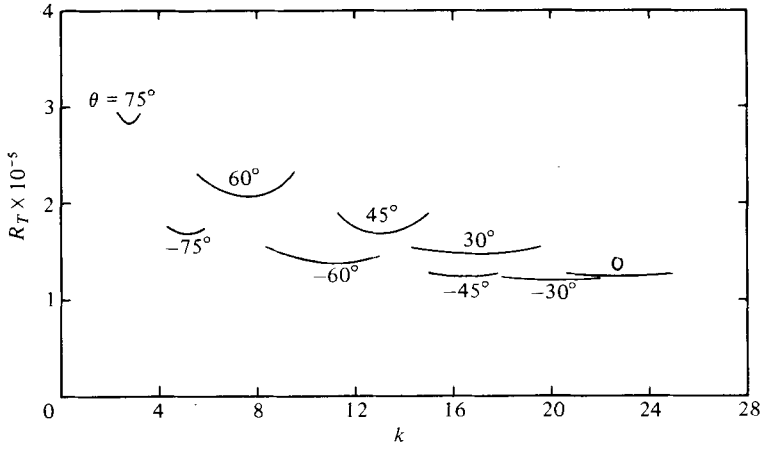

FIGURE 10. Natural stability curves at various inclination angles.

theoretical curve (figure 9) is also a likely situation. Layer thicknesses are measured from shadowgraphs taken about 3–5 min after the onset of instability. During this time, the layers continuously grow in size, and it is therefore very likely that the measured wavelengths are larger (or the wavenumber, $k_c = 2\pi/\lambda_c$, is smaller). Considering these experimental uncertainties, the agreement of theoretical predictions with experiments is excellent.

It is interesting to note that the neutral stability curve is very flat near the critical state at $\theta = 0°$ as shown in figure 10. As the magnitude of θ increases, the critical wavenumber becomes more and more sharply defined. This is the result of the effect of the angle of inclination. Since the horizontal temperature gradient is the destabilizing agent, a larger ΔT is needed to obtain the same destabilizing effect as the angle of inclination is increased. The sharper definition of the critical wavelength in the $\theta > 0$ cases can be explained by the fact that the flow is more stable in this case as explained below.

In I, we presented a physical argument involving the increased vertical solute

gradient which explains the enhanced stability when the lower wall is heated. In the following, we present an analytic derivation of the density gradients, both in the horizontal and vertical directions, due to temperature and salt, separately. These results will support our earlier physical reasoning.

The essential condition that must always be satisfied by the basic state in the fluid interior is that the horizontal density gradients due to S and T are compensating, that is

$$\alpha \frac{\partial T'}{\partial \xi'} = \beta \frac{\partial S'}{\partial \xi'}.$$

With transformation of co-ordinates and non-dimensionalization of the variables, the horizontal and vertical gradients of S and T can be written as:

$$\frac{\partial S}{\partial \xi} = \left(\frac{dS}{dx} + \sin\theta\right)\cos\theta, \quad \frac{\partial T}{\partial \xi} = -\cos\theta;$$

$$\frac{\partial S}{\partial \zeta} = \left(\frac{dS}{dx}\sin\theta - \cos^2\theta\right), \quad \frac{\partial T}{\partial \zeta} = -\sin\theta.$$

These equations are dimensionalized and integrated. Contributions to the net fluid density due to solute and due to temperature are computed in the horizontal and vertical directions. Fractional density distributions $((\rho-\rho_0)/\rho_0)$ are plotted in figures 11 and 12; ρ_0 is the reference fluid density at the centre of the slot.

Figure 11 shows the steady-state distribution of density due to solute $((\rho_S-\rho_0)/\rho_0)$ and that due to temperature $((\rho_T-\rho_0)/\rho_0)$ in the horizontal direction. It should be noticed that horizontal width of the slot is a function of θ. For a given temperature difference across the walls, horizontal width of the slot increases with $|\theta|$ and hence the magnitude of the gradients decreases. Except near the walls, the density gradients due to temperature and solute are always equal and opposite. For a fixed inclination, the magnitudes of the gradients increase as R_T increases. For $\theta \neq 0°$ the magnitudes of horizontal gradients decrease as θ increases, for the same R_T. R_T, therefore, has to be sufficiently increased before the horizontal gradients attain magnitudes conducive to triggering of instability at relatively higher $|\theta|$ values.

Figure 12 shows the steady-state fractional density distribution due to the solute $((\rho_S-\rho_0)/\rho_0)$ and due to temperature $((\rho_T-\rho_0)/\rho_0)$ in the vertical direction for $\theta = 0°$, $\pm 30°$ and $\pm 60°$ and $R_T = 0$ and 100000. The actual vertical distance between the boundaries is 2·0 cm for $\theta = \pm 30°$ and 1·154 cm for $\theta = \pm 60°$, as shown in the figure. It is noticed that the total vertical density gradient, in general, consists of the density gradient due to solute plus that due to temperature. The net gradient is always equal to its initial value, and is stabilizing in nature. For positive angles (lower wall heated), as the destabilizing density gradient due to the vertical component of the temperature gradient develops, the stabilizing vertical gradient due to solute increases by the same amount, and thus the net gradient remains unchanged. At negative angles (upper wall heated), heating provides part of the total vertical stabilizing effect originally provided by the solute alone. No vertical density gradient due to temperature ever exists in the case of $\theta = 0°$, and therefore the net density gradient is always due to solute alone. Although the net stable vertical gradient retains its initial value, the ratio of $|dS/d\zeta|$ at steady state to $|dS/d\zeta|_0$ is minimum for $\theta = -75°$, equals 1 for $\theta = 0°$ and is

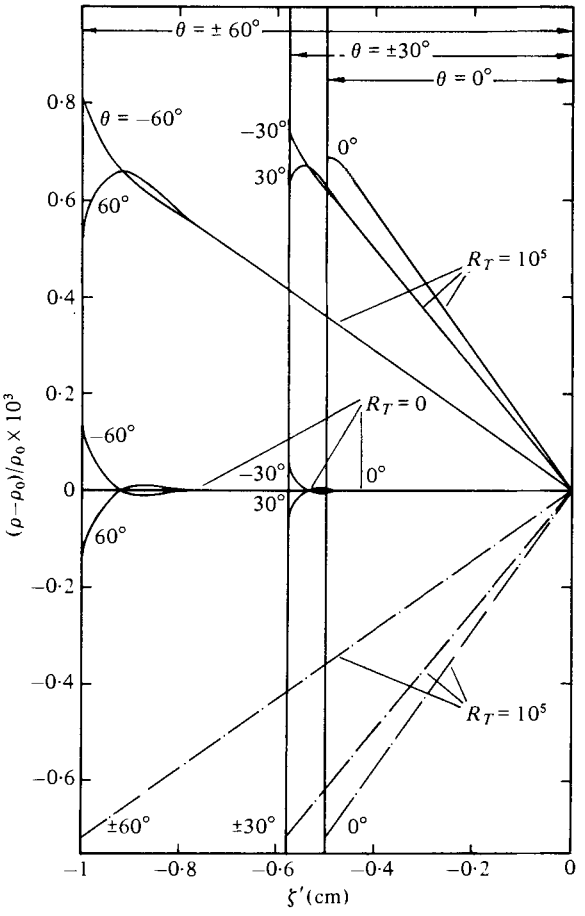

FIGURE 11. Steady-state distribution of density due to solute and due to temperature in the horizontal direction. ——, $(\rho_S-\rho_0)/\rho_0$; —·—, $(\rho_T-\rho_0)/\rho_0$.

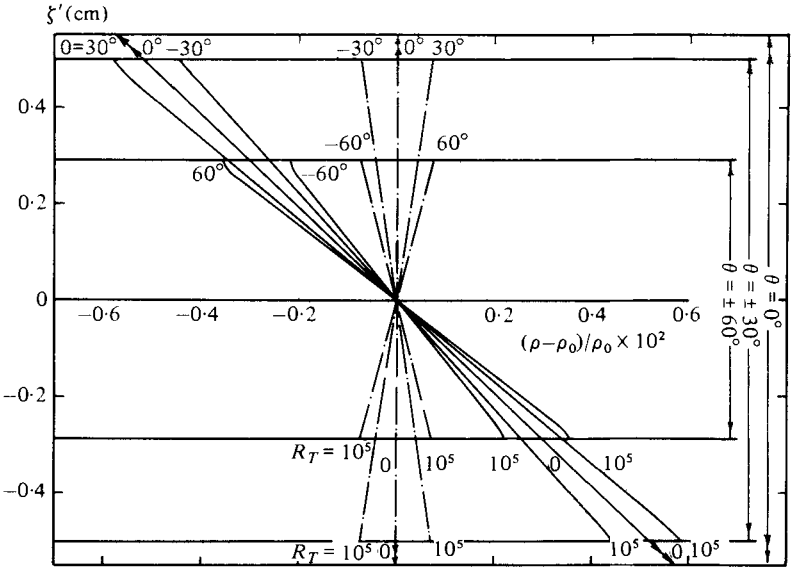

FIGURE 12. Steady-state distribution of density due to solute and due to temperature in the vertical direction. ——, $(\rho_S-\rho_0)/\rho_0$; —·—, $(\rho_T-\rho_0)/\rho_0$.

maximum for $\theta = +75°$, for the same amount of heating. Since the sideways double-diffusive instability observed in the experiments involves heated parcels of fluid rising against the background solute gradient, the steady state showing the larger solute gradient will be more stable.

The financial support of the National Science Foundation through Grant ENG 73-03545-A01 is gratefully acknowledged.

REFERENCES

FINLAYSON, B. A. 1972 *The Method of Weighted Residuals and Variational Principles*, pp. 151–203. Academic.

HART, J. E. 1970 Thermal convection between sloping parallel boundaries. Ph.D. thesis, Massachusetts Institute of Technology.

HART, J. E. 1971*a* Stability of the flow in a differentially heated inclined box. *J. Fluid Mech.* **47**, 547–576.

HART, J. E. 1971*b* On sideways diffusive instability. *J. Fluid Mech.* **49**, 279–288.

HART, J. E. 1973 Finite amplitude sideways diffusive convection. *J. Fluid Mech.* **59**, 47–64.

PALIWAL, R. C. 1979 Double-diffusive convective instability in an inclined fluid layer. Ph.D. thesis, Department of Mechanical, Industrial and Aerospace Engineering, Rutgers University.

PALIWAL, R. C. & CHEN, C. F. 1980 Double-diffusive instability in an inclined fluid layer. Part 1. Experimental investigation. *J. Fluid Mech.* **98**, 755–768.

SHIRTCLIFFE, T. G. L. 1969 An experimental investigation of thermosolutal convection at marginal stability. *J. Fluid Mech.* **35**, 677–688.

THORPE, S. A., HUTT, P. K. & SOULSBY, R. 1969 The effect of horizontal gradients on thermohaline convection. *J. Fluid Mech.* **38**, 375–400.

VERONIS, G. 1965 On finite amplitude instability in thermohaline convection. *J. Mar. Res.* **23**, 1–17.